NeuroToxicology 30 (2009) 915–925

Contents lists available at ScienceDirect

NeuroToxicology

Mild steel welding fume causes manganese accumulation and subtle neuroinflammatory changes but not overt neuronal damage in discrete brain regions of rats after short-term inhalation exposure

James M. Antonini *, Krishnan Sriram, Stanley A. Benkovic, Jenny R. Roberts, Samuel Stone, Bean T. Chen, Diane Schwegler-Berry, Amy M. Jefferson, Brenda K. Billig, Christopher M. Felton, Mary Ann Hammer, Fang Ma, David G. Frazer, James P. O'Callaghan, Diane B. Miller

Health Effects Laboratory Division, National Institute for Occupational Safety and Health, Morgantown, WV 26505, USA

ARTICLE INFO

Article history:
Received 15 May 2009
Accepted 17 September 2009
Available online 25 September 2009

Keywords:
Welding fume
Inhalation
Manganese
Neuroinflammation
Gliosis
Manganism
Dopaminergic neurotoxicity

ABSTRACT

Serious questions have been raised by occupational health investigators regarding a possible causal association between neurological effects in welders and the presence of manganese (Mn) in welding fume. Male Sprague–Dawley rats were exposed by inhalation to 40 mg/m^3 of gas metal arc-mild steel (MS) welding fume for 3 h/day for 10 days. Generated fume was collected in the animal chamber during exposure, and particle size, composition, and morphology were characterized. At 1 day after the last exposure, metal deposition in different organ systems and neurological responses in dopaminergic brain regions were assessed in exposed animals. The welding particles were composed primarily of a complex of iron (Fe) and Mn and were arranged as chain-like aggregates with a significant number of particles in the nanometer size range. Mn was observed to translocate from the lungs to the kidney and specific brain regions (olfactory bulb, cortex, and cerebellum) after MS fume inhalation. In terms of neurological responses, short-term MS fume inhalation induced significant elevations in divalent metal ion transporter 1 (Dmt1) expression in striatum and midbrain and significant increases in expression of proinflammatory chemokines (Ccl2, Cxcl2) and cytokines (IL1β, TNFα) in striatum. In addition, mRNA and protein expression of glial fibrillary acidic protein (GFAP) was significantly increased in striatum after MS fume exposure. However, the 10-day MS welding fume inhalation did not cause any changes in dopamine and its metabolites or GABA in dopaminergic brain regions nor did it produce overt neural cell damage as assessed by histopathology. In summary, short-term MS welding fume exposure led to translocation of Mn to specific brain regions and induced subtle changes in cell markers of neuroinflammatory and astrogliosis. The neurofunctional significance of these findings currently is being investigated in longer, more chronic welding fume exposure studies.

Published by Elsevier Inc.

1. Introduction

Hundreds of thousands of workers in the United States (Bureau of Labor Statistics, 2007) and millions of workers worldwide are exposed to welding aerosols on a daily basis. Welding fume is a complex mixture composed of different metals, predominantly iron (Fe). Most welding fumes contain a small percentage of manganese (Mn) that is complexed with other metals. The amount of Mn in the generated fume may vary due to the type of welding process or rod/electrode that are used. Serious questions have been raised by occupational health officials regarding a possible causal association between reported neurological effects in welders and the presence of Mn in welding fume. Unfortunately, most studies of welders' health have examined the respiratory effects (Antonini, 2003). Less

Abbreviations: α2m, alpha 2 microglobulin; Ccl2, chemokine–chemokine ligand 2; Cxcl2, chemokine-X-chemokine ligand 2; CNS, central nervous system; ELISA, enzyme-linked immunosorbent assay; Actb, beta actin; GFAP, glial fibrillary acidic protein; Glul, glutamine synthetase; Glast, glutamate transporter; IL1α, interleukin 1 alpha; IL1β, interleukin 1 beta; IL6, interleukin 6; PCR, polymerase chain reaction; PD, Parkinson's disease; SDS, sodium dodecyl sulfate; TNF, tumor necrosis factor; Dmt1, divalent metal transporter 1; Trf, transferrin; OB, olfactory bulb; STR, striatum; MB, midbrain; GP, globus pallidus; HIP, hippocampus; CTX, cortex; CER, cerebellum; TH, thalamus; MMAD, mass median aerodynamic diameter; MOUDI, Micro-Orifice Uniform Deposit Impactor; SEM, scanning electron microscopy; ICP-AES, inductively coupled plasma atomic absorption spectroscopy; TEM, transmission electron microscopy; MS, mild steel; NADH, nicotinamide adenine dinucleotide; Iba-1, ionized calcium binding adapter molecule 1.

* Corresponding author at: Health Effects Laboratory Division, National Institute for Occupational Safety and Health, 1095 Willowdale Road, Mailstop 2015, Morgantown, WV 26505, USA. Tel.: +1 304 285 6244; fax: +1 304 285 5938.
E-mail address: jga6@cdc.gov (J.M. Antonini).

0161-813X/$ – see front matter. Published by Elsevier Inc.
doi:10.1016/j.neuro.2009.09.006

information exists about the potential neurological effects associated with welding and the biological fate of Mn after inhalation of welding fume (Antonini et al., 2006a).

The health of welders has been a challenge to study due to diverse workplace settings and exposure to complex and varied aerosols generated from a multitude of welding processes. Welders may work in a variety of settings that can include open, well-ventilated spaces (e.g., outdoor construction site) or enclosed, poorly ventilated spaces (e.g., ship hull, crawl space, holding tank). Several case reports of suspected Mn overexposure in welders have been reported (Wang et al., 1989; Franek, 1994), and a positive brain magnetic resonance imaging (MRI) T1 hyperintensity signal in the globus pallidus, indicative of Mn accumulation, has been observed in some studies (Nelson et al., 1993; Kim et al., 1999, 2005; Discalzi et al., 2000; Sadek et al., 2003; Josephs et al., 2005).

Mn overexposure or "manganism" is a neurological syndrome characterized by central nervous system abnormalities and neuropsychiatric disturbances that are similar and have some symptoms in common with Parkinson's disease (PD). Both conditions are characterized by generalized bradykinesia and widespread rigidity, but are differentiated based on their clinical, pharmacological, imaging, and pathological profiles (Calne et al., 1994; Perl and Olanow, 2007). The similarities of the two disorders may be explained by the fact that in manganism the basal ganglia accumulate most of the excess Mn compared to other brain regions, and dysfunction in the basal ganglia is also the basis of Parkinson's disease (Dobson et al., 2004). However, Parkinson's disease is primarily associated with the loss of dopaminergic neurons within the substantia nigra (Pal et al., 1999; McMillan, 1999). The substantia nigra is spared in manganism, which is linked to the degeneration of intrinsic neurons within the globus pallidus.

The knowledge that exposure to high levels of manganese results in the defined neurological condition of manganism has caused some to express concern about the risk for neurological disease in those workers, including welders, who experience repeated low dose exposures to this metal (NIOSH, 2009). One case–control study has suggested that exposure to welding fume may accelerate the onset of idiopathic PD (Racette et al., 2001), but this study has been criticized for accepting co-existence as sufficient evidence for a relationship (Jankovic, 2005). In a death certificate-based study of neurodegenerative diseases, an excess in mortality due to idiopathic PD was observed in those under 65 whose occupation included welding (Park et al., 2005), but recent work (Stampfer, 2009) suggests the observed association with age may not be due to an increase in risk among young men but rather a reduced likelihood of a PD death being associated with welding in those men dying at an older age. Also, other mortality survey studies and epidemiological studies have not found an association between welding and PD or other neurodegenerative conditions (Coggon et al., 1995; Fored et al., 2006; Fryzek et al., 2005; Goldman et al., 2005; Lehman et al., 2008; Marsh and Gula, 2006; Park et al., 2006).

Other population-based surveys and cross-sectional studies of welders exposed to welding fume containing Mn have identified subtle neurological and neuropsychological changes, compromised psychomotor and motor function, and some cognitive difficulties (Sinczuk-Walczak et al., 2001; Sjogren et al., 1990, 1996; Bowler et al., 2003, 2007a, 2007b; Kim et al., 2005; Ellingsen et al., 2008). Unfortunately, the clinical significance of these reported neurological symptoms in welders is unknown. Studies investigating the progression of these symptoms have not been reported and make it difficult to know if such symptoms are predictive of later disease. Of most concern in determining the significance of the reported effects is the lack of detailed and accurate exposure information about all aspects of the welding exposure including the processes and types of rods/wires used, fume and Mn concentrations, duration and frequency of welding, as well as exposure to the other neurotoxicants found in welding fumes.

As exposures can be strictly controlled in animal studies, it was our goal to develop an animal model to mimic human exposure conditions to welding fumes and determine the neural consequences of exposure. Primarily, our effort was to address the following questions: (1) do metals, in particular Mn, that are deposited in the respiratory tract after welding fume exposure translocate to extrapulmonary organ systems?; (2) if so, what are the possible mechanisms of translocation (e.g., olfactory uptake, transepithelial transport of welding nanoparticles to the circulation, lymphatic clearance)?; (3) is it possible to elicit systemic responses outside the pulmonary system after welding fume inhalation? Here, we describe a preliminary study that uses a novel robotic welder developed by NIOSH to perform short-term inhalation exposures of laboratory animals to a high concentration of mild steel (MS) welding fume, the most common type in U.S. industry. The metals that are present in MS fume were measured in different organs to assess their translocation from the respiratory tract to other organ systems, with a focus on the central nervous system (CNS). In addition, histopathological assessment of neuronal cell damage and biochemical and molecular indices of neuroinflammation and gliosis were measured in discrete brain regions to examine potential systemic effects after welding fume inhalation.

2. Materials and methods

2.1. Experimental design

Rats were exposed by inhalation to 40 mg/m^3 of MS welding fume for 3 h/day for 10 days. At 1 day after the last exposure, neurological responses, pulmonary injury and inflammation, and metal deposition in different organ systems were assessed in exposed animals. A target MS fume exposure concentration of 40 mg/m^3 was chosen for study. It was our goal to generate a high enough exposure fume concentration that would lead to significant particle/metal load in the lungs, but without the presence of lung injury or inflammation. A complete analysis of the pulmonary effects of inhaled MS fume at the concentration used in this study has been reported previously and observed not to induce lung injury or inflammation (Antonini et al., 2009). After exposure, separate sets of animals from each treatment group were euthanized by either sodium pentobarbital overdose for RNA and protein analyses or by focused microware irradiation for measurement of neurotransmitters, as described under related methods.

2.2. Welding fume generation system

The welding fume generation system consisted of a welding power source (Power Wave 455, Lincoln Electric, Cleveland, OH, USA), an automated, programmable six-axis robotic arm (Model 100 Bi, Lincoln Electric, Cleveland, OH, USA), and a water-cooled arc welding torch (WC 650 A, Lincoln Electric, Cleveland, OH, USA) as previously described (Antonini et al., 2006b). Gas metal arc welding was performed using a mild steel electrode (carbon steel ER70S-6, Lincoln Electric, Cleveland, OH, USA). Welding took place on A36 carbon steel plates for daily exposures of 3 h at 25 V and 200 A. During welding, a shielding gas combination of 95% Ar and 5% CO_2 (Airgas Co., Morgantown, WV, USA) was continually delivered to the welding nozzle at an air flow rate of 20 L/min.

2.3. Exposure chamber fume and gas determinations

A flexible trunk was positioned approximately 18 in. from the arc to collect the generated fume and transport it to the exposure chamber. The generated welding fume was mixed with dry HEPA-filtered air. Continuous records of chamber fume concentration, temperature, and humidity were maintained during welding fume generation. Fume was collected onto 37-mm Teflon filters at a rate of 1 L/min, and the particle mass delivered to the exposure chamber was determined gravimetrically every 30 min in duplicate during the daily 3-h exposure. Rats were exposed to a target concentration of 40 mg/m^3 for 3 h/day for 10 days. Actual daily fume concentrations (mg/m^3) were (34.1, 38.7, 43.0, 39.5, 44.9, 43.0, 43.0, 32.6, 45.3, and 44.6) with a measured mean of 40.9 $\pm$ 7.6 mg/m^3 SD. In addition, particle samples were periodically collected gravimetrically onto grids for electron microscopy to assess particle size distribution, particle morphology, and elemental composition.

2.4. Welding particle characterization

Particle size distribution was determined by using a Micro-Orifice Uniform Deposit Impactor (MOUDI, MSP Model 110, MSP Corporation, Shoreview, MN, USA) and a Nano-MOUDI (MSP Model 115). Using the two MOUDI impactors, it was possible to collect particles in the size range from 0.01 to 18 μm that were separated into 15 fractions. Welding fume samples were collected at 30-min intervals during 3 h of welding directly onto formvar-coated TEM grids on different stages of the MOUDI impactors and viewed using a JEOL 1220 transmission electron microscope (JEOL, Inc., Tokyo, Japan).

To determine elemental composition, additional welding particles were collected onto 5.0 μm polyvinyl chloride membrane filters in 37-mm cassettes. The particle samples were digested and the metals analyzed by inductively coupled plasma atomic emission spectroscopy (ICP-AES) by the Division of Applied Research and Technology (DART, Cincinnati, OH) according to NIOSH method 7300 (NIOSH, 1994). In addition, the water solubility of the MS welding fume was determined. The MS welding fume sample was suspended in distilled water, pH 7.4, and sonicated for 1 min with a Sonifier 450 Cell Disruptor (Branson Ultrasonics, Danbury, CT, USA). The particle suspension (total samples) was incubated for 24 h at 37 °C, and the sample was centrifuged at 12,000 $\times$ *g* for 30 min. The supernatant of the sample (soluble fraction) was recovered and filtered with a 0.22 μm filter (Millipore Corp., Bedford, MA, USA). The pellet (insoluble fraction) was resuspended in water. The samples (total, soluble, and insoluble fractions) were digested, and the metals analyzed by ICP-AES. The MS fume was found to be highly insoluble in water with a soluble/insoluble ratio of 0.0139.

2.5. Animals

Male Sprague–Dawley [Hla:(SD) CVF] rats from Hilltop Lab Animals (Scottdale, PA, USA), weighing 250–300 g and free of viral pathogens, parasites, mycoplasmas, Helicobacter, and CAR Bacillus, were used for all exposures. The rats were acclimated for at least 6 days after arrival and were housed in ventilated polycarbonate cages on Alpha-Dri cellulose chips and hardwood beta-chips as bedding, and provided HEPA-filtered air, irradiated Teklad 2918 diet, and tap water *ad libitum* when not being exposed. The animal facilities are specific pathogen-free, environmentally controlled, and accredited by the Association for Assessment and Accreditation of Laboratory Animal Care International (AAALAC). All animal procedures used during the study were reviewed and approved by the NIOSH Animal Care and Use Committee.

During the daily 3-h exposures to welding fume or air while in the inhalation chamber, food and water were withheld from the animals. Body weight was monitored before and after each exposure. No significant changes were observed in animal body weight for either treatment group during the exposure regimen used in the study (data not shown). In addition, during exposure to MS welding fume, no animal showed any outward signs of labored breathing or respiratory distress. Respiratory rate was not significantly different when comparing fume-exposed and air control animals (data not shown).

2.6. Tissue deposition of metals

Non-lavaged left lungs, brain regions [left hippocampus (HIP), left cerebellum (CER), left striatum (STR), left thalamus (TH), left cortex (CTX), left olfactory bulb OB), and left midbrain (MB)], heart, liver, kidney, spleen, and whole blood were collected from exposed animals and freeze-dried after lyophilization. The dried tissue and blood samples were digested in a microwave in the presence of nitric acid. The amount of Fe, Mn, Cu, Al, Cr, Ni, Ti, V, and Zn present in the samples was determined by ICP-AES at NIOSH-DART (Cincinnati, OH), according to NIOSH method 7300 (NIOSH, 1994). No significant differences in blood and tissue levels for Al, Cr, Ni, Ti, V, and Zn were measured between the two groups.

2.7. Biochemical and molecular parameters of neural injury

At 1 day after the last exposure, animals were anesthetized with an intraperitoneal injection of sodium pentobarbital (>100 mg/kg body weight; Sleepaway, Fort Dodge Animal Health, Wyeth, Madison, NJ, USA) and exsanguinated. Brains were excised and brain areas (olfactory bulb, striatum, globus pallidus, hippocampus, frontal cortex, cerebellum, thalamus, and midbrain) from the left and right hemispheres were dissected free-hand. Brain regions from the left hemisphere were placed in RNA*later*® (Ambion, Austin, TX, USA) for mRNA expression analysis and tissues from the right hemisphere were processed in 10 volumes of hot (85–95 °C) 1% SDS for analysis of proteins.

2.7.1. RNA isolation, cDNA synthesis and real-time PCR

The tissues (olfactory bulb, striatum and midbrain) were homogenized in Tri Reagent® (Molecular Research Center, Inc., Cincinnati, OH, USA) and the aqueous phase separated with MaXtract High Density gel (Qiagen, Valencia, CA, USA). Total RNA from the aqueous phase was then isolated using RNeasy mini spin columns (Qiagen, Valencia, CA, USA), DNase treated and the concentrations were determined with a NanoDrop® ND-1000 UV–vis Spectrophotometer (NanoDrop Technologies, Wilmington, DE, USA).

First strand cDNA synthesis was carried out using total RNA (1 μg), random hexamers and MultiScribe™ reverse transcriptase (Applied Biosystems, Foster City, CA, USA) in a 20 μl reaction. Real-time PCR amplification was performed using the 7500 Real-Time PCR System (Applied Biosystems, Foster City, CA, USA) in combination with TaqMan® chemistry. Specific primers and FAM™ dye-labeled TaqMan® MGB probe sets (TaqMan® Gene Expression Assays) for Ccl2, Cxcl2, IL1α, IL1β, IL6, TNFα, α2m, GFAP, Glul, Glast, Dmt1, Trf and Actb (endogenous control), were procured from Applied Biosystems (Foster City, CA) and used according to the manufacturer's recommendation. All PCR amplifications (40 cycles) were performed in a total volume of 25 μl, containing 1 μl cDNA, 2.5 μl of the specific TaqMan® Gene Expression Assay and 20 μl of TaqMan® Universal master mix (Applied Biosystems, Foster City, CA, USA), respectively. Sequence detection software (version 1.7; Applied Biosystems, Foster City, CA) results were exported as tab-delimited text files and imported

into Microsoft Excel for further analysis. Relative quantification of gene expression was performed using the comparative threshold (C_T) method as described by the manufacturer (Applied Biosystems, Foster City, CA; User Bulletin 2). Changes in mRNA expression were calculated following normalization to endogenous control and are expressed as fold change over air-exposed controls.

2.7.2. GFAP ELISA

GFAP was assayed in accordance with a previously described procedure (O'Callaghan, 1991, 2002). In brief, a rabbit polyclonal antibody to GFAP was coated on the wells of Immulon-2 microtiter plates (Thermo Labsystems, Franklin, MA, USA). The SDS homogenates and standards were diluted in phosphate-buffered saline (pH 7.4) containing 0.5% Triton-X 100 solution. After blocking nonspecific binding with 5% non-fat dry milk, aliquots of the homogenate and standards were added to the wells and incubated. Following washes, a mouse monoclonal antibody to GFAP was added to "sandwich" the GFAP between the two antibodies. An alkaline phosphatase conjugated antibody directed against mouse IgG was then added and a colored reaction product was obtained by subsequent addition of the enzyme substrate, p-nitrophenol. Quantification was achieved by spectrophotometry of the colored reaction product at 405 nm in a microplate reader, Spectra Max Plus and analyzed with Soft Max Pro Plus software (Molecular Devices, Sunnyvale, CA, USA). The amount of GFAP in the samples was calculated as μg GFAP/mg total protein and the data are expressed as percent of air control.

2.8. Analysis of the levels of dopamine and its metabolites

For the analysis of dopamine and its metabolites, the animals were euthanized by focused microwave irradiation (power level of 4 kW and exposure time of 0.9 s) using a microwave applicator (Muromachi Kikai, Inc, Tokyo, Japan; model TMW-4012C). This method of euthanasia is approved by the Panel on Euthanasia of the American Veterinary Medical Association (AVMA, 2001). Following euthanasia, the brains were excised, and brain areas (olfactory bulb, striatum, globus pallidus, hippocampus, frontal cortex, cerebellum, thalamus, and midbrain) were free-hand dissected from both hemispheres. Tissue remained frozen at −80 °C until prepared for assay.

Dopamine (DA) and its metabolites were quantified by high-performance liquid chromatograph with electrochemical detection (HPLC-EC). Tissues were homogenized in 100 μl of ice-cold 0.2 M perchloric acid, containing 1 μM dihydroxybenzylamine as internal standard, and centrifuged at 10,000 × *g* for 10 min at 4 °C. The supernatant was filtered through a 0.2 μm membrane, and an aliquot (10 μl) was injected from a temperature-controlled (4 °C) automatic sample injector (Waters 717plus Autosampler) connected to a Waters 515 HPLC pump. Catecholamines were separated on a C18 reverse-phase column (LC-18 RP; Waters SYMMETRY 25 cm × 4.6 mm; 5 μm), electrochemically detected (Waters 464 Pulsed Electrochemical Detector; range 10 nA, potential +0.7 V), and analyzed using Millennium software. The mobile phase, pH 3.0, for isocratic separation of DA consisted of dibasic sodium phosphate (75 mM), octane sulfonic acid (1.7 mM), acetonitrile (10%, v/v), and EDTA (25 μM). Flow rate was maintained at 1 ml/min. DA, 3,4-dihydroxyphenylacetic acid (DOPAC), and homovanillic acid (HVA) standards (0.5–25 pmol) were prepared in 0.2 M perchloric acid containing dihydroxybenzylamine. Recovery of each analyte was adjusted with respect to the internal standard and quantified from a standard curve. The levels of DA and its metabolites, DOPAC and HVA, were calculated as μg/g wet weight and are expressed as percent of saline control.

2.9. Animal preparation for determination of neuropathology

A separate set of treated rats were deeply anesthetized with sodium pentobarbital (>100 mg/kg body weight; Sleepaway, Fort Dodge Animal Health, Wyeth, Madison, NJ, USA), and were perfused transcardially with 150 ml of ice-cold saline followed by 250 ml of perfusion solution (4.0% paraformaldehyde in Sorensen's phosphate buffer). Brains were removed, incubated in fixative overnight, and cryoprotected serially in 10%, 20%, and 30% sucrose in Dulbecco's modified phosphate-buffered saline (DPBS) for 24 h each. Brains were embedded in OCT (Tissue Tek, Zoeterwoude, The Netherlands), sectioned in the horizontal plane at 35 μm on a Lecia cryostat (Model CM3000, Meyer Instruments, Houston, TX, USA), and stored in DPBS containing 0.8 g/L sodium azide. These brains were sectioned completely through the horizontal plane. Twelve sections per brain were processed for each stain (every sixth section through the areas of interest).

2.10. Fluoro-Jade B staining

Selected brain sections were stained with Fluoro-Jade B, a fluorescent marker for the localization of degenerating neurons, using a slightly modified procedure (Schmued and Hopkins, 2000). Unstained sections were mounted onto Colorfrost microscope slides (Fisher, Pittsburgh, PA, USA), and were allowed to air dry overnight. Slides were dipped in distilled water twice, and placed into 70% ethanol for 2 min, followed by distilled water for 2 min. Background staining was suppressed by incubation in 0.06% potassium permanganate for 15 min with shaking. A rinse in distilled water for 2 min was followed by immersion in the staining solution for 20 min (0.01% stock solution, 4 ml of stock solution diluted in 96 ml of 0.1% acetic acid). After staining, slides were washed three times in distilled water for 1 min each, and were allowed to air dry overnight. Slides were placed on a warmer at 55 °C for 5 min, transferred to 100% ethanol for 5 min, cleared in xylene for 5 min, and coverslipped with DPX (Fluka, Sigma–Aldrich, St. Louis, MO, USA).

2.11. Immunohistochemistry

To visualize GFAP and Iba-1 immunoreactivity, brain sections were stained free-floating using a modified ABC procedure (Vector Laboratories, Burlingame, CA, USA). Sections were treated with 10% methanol, 10% hydrogen peroxide in DPBS for 15 min to quench endogenous peroxidase. Following three rinses in DPBS for 5 min each, sections were incubated in a permeabilizing solution (1.8% L-lysine, 4% normal horse serum, 0.2% Triton-X 100 in DPBS) for 30 min at room temperature. Sections were transferred directly to primary antibody solution in DPBS with 4% horse serum (rabbit anti-cow GFAP, 1:10,000, Dako, Glostrup, DK; rabbit anti-Iba-1, 1:500, Wako, Richmond, VA, USA) and were incubated overnight at room temperature. The following day, sections were rinsed three times in DPBS for 5 min each, and transferred to secondary antibody solution in DPBS with 4% horse serum (anti-rabbit IgG, 1:10,000, Vector Laboratories, Burlingame, CA, USA; anti-rabbit IgG, 1:500, Vector Laboratories, Burlingame, CA) for 2 h at room temperature. Following three rinses in DPBS, sections were incubated in Avidin D-HRP (Vector Laboratories, 1:1000 in DPBS) for 1 h at room temperature, rinsed three times in DPBS, and incubated with chromagen solution DAB (for GFAP, 25 mg/50 ml DPBS + 50 μl 30% hydrogen peroxide, Sigma, St. Louis, MO, USA) or Nova Red (for Iba-1, Vector Laboratories, Burlingame, CA, USA) for 5 min. Following a 5-min rinse (DPBS for GFAP, distilled water for Iba-1), sections were mounted onto microscope slides (Colorfrost+, Fisher), air-dried overnight, dehydrated through a standard ethanol series, and coverslipped with Permount (Fisher, Pittsburgh, PA, USA).

2.12. Microscopy

Microscopic analysis of stained brain sections was performed at NIOSH on an Olympus BX-50 microscope (Olympus America, Center Valley, PA, USA) interfaced with a Spot II digital camera (Diagnostic Instruments Inc., Sterling Heights, MI, USA) controlled by a Macintosh G4 computer (Apple Computer Inc., Cupertino, CA, USA). Images were captured with Spot software (v4.5) and assembled and labeled in Adobe Photoshop CS2 (Adobe Systems Inc., San Jose, CA, USA).

2.13. Statistical analysis

Results are expressed as means ± standard error of measurement. Statistical analysis was performed using JMP statistical software (SAS, Inc., Belmont, CA, USA). Analyses of the data were performed to determine that the values for the treatment groups were normally distributed and had the same variance. The significance of difference between welding fume exposure and controls group was analyzed using an unpaired student's *t*-test. For all analyses, the criterion of significance was set at $p < 0.05$.

3. Results

3.1. Welding fume characterization

Table 1 illustrates the metal profile of the generated MS welding fume collected in the breathing zone of the animals. The particles were found to be highly water-insoluble and composed primarily of Fe (80.6%), Mn (14.7%), Si (2.75%), and Cu (1.79%). Airborne MS welding fume was collected onto different stages of a Nano-MOUDI sampler and analyzed by TEM. The vast majority of the mass of the particles was observed to be in the fine size cut-off range of 0.10–1.0 μm (data not shown). The mass median aerodynamic diameter (MMAD) was determined to be approximately 0.31 μm. Many particles were observed in the ultrafine size range below 0.10 μm. Particles were arranged as typical chain-like aggregates commonly produced by gas metal arc welding processes (Fig. 1). Numerous nanometer-sized agglomerates (<0.10 μm) were observed on different stages of the Nano-MOUDI sampler (Fig. 1B–D), giving a significant number of particles a higher probability of translocating from pulmonary structures to the circulation and other organ systems.

Table 1
Metal composition of generated mild steel welding fume.

Metals	Sample (μg)	Weight % of metals[a]
Fe	776 ± 9.8	80.6 ± 0.17
Mn	142 ± 2.0	14.7 ± 0.11
Si	26.6 ± 2.9	2.75 ± 0.28
Cu	17.2 ± 0.20	1.79 ± 0.02

Note. Values are means ± standard error; $n = 5$ welding collection periods of 30 min.
[a] Relative to all metals analyzed. Trace amounts (<0.02 wt. %) of Al, Cr, Ni, and Ti also were present. The data in this table has been previously presented (Antonini et al., 2009).

3.2. Pulmonary metal deposition

Significant elevations in Fe, Mn, and Cu were observed in lungs after 10 days of exposure to MS welding fume compared to air control (Table 2). Despite the relatively high MS welding fume concentration used, no evidence of lung inflammation, as

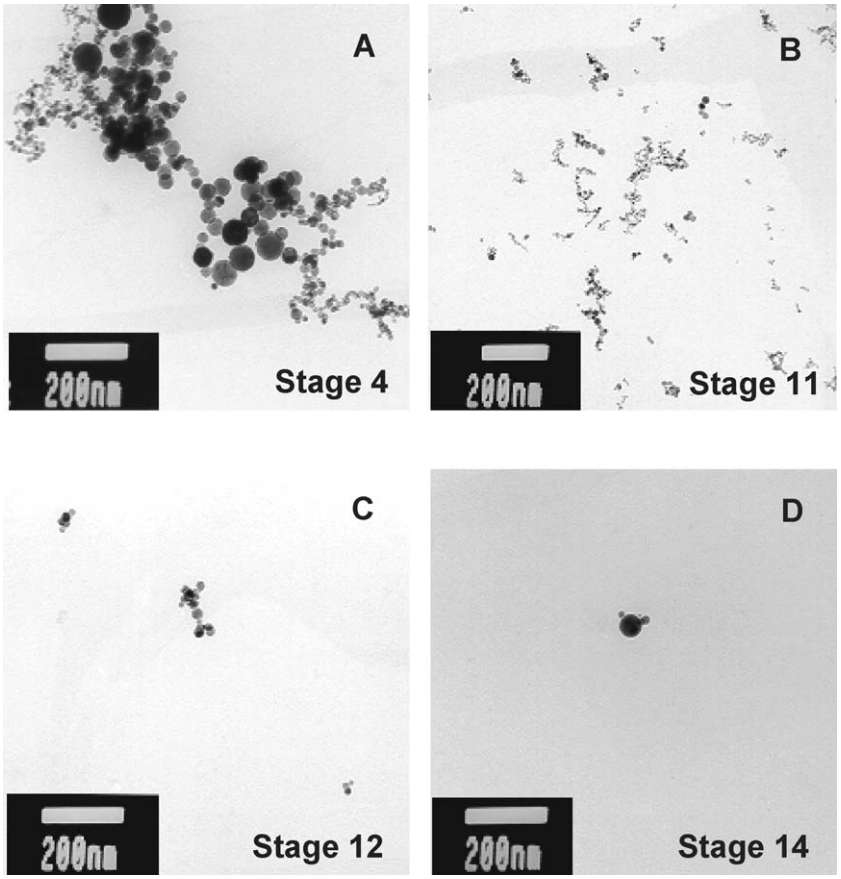

Fig. 1. Representative transmission electron micrographs of mild steel welding particles on: (A) stage 4; (B) stage 11; (C) stage 12; (D) stage 14 of the aerosol sampler. Note the presence of nanometer-sized (<0.1 μm) agglomerates generated during welding on stages 12 and 14 of the particle impactor.

Table 2
Lung metal deposition and toxicity profile.

Group	Fe (μg/g dry tissue)	Mn (μg/g dry tissue)	Cu (μg/g dry tissue)
Air	418 ± 40.7	0.66 ± 0.04	5.73 ± 0.17
Mild Steel WF	1509 ± 176[a]	98.3 ± 10.5[a]	11.3 ± 1.27[a]

Note. Pulmonary deposition of Fe, Mn, and Cu at 1 day after inhalation of 40 mg/m^3 of mild steel welding fume (WF) for 3 h/day for 10 days. Control animals were exposed to filtered air. Values are means ± standard error (n = 5–6).
[a] Significantly greater than corresponding air control for a particular metal, $p < 0.05$.

determined by PMN influx, or injury, as determined by LDH and albumin measurements, was observed after the 10-day exposure (as previously reported in Antonini et al., 2009).

3.3. Blood and non-target tissue metal deposition

A slight, but not significant, increase in Mn was measured in whole blood of animals exposed to the MS welding fume (Table 3). In nearly every case, there was a slight increase in Fe and Mn measured in the liver, heart, kidney, and spleen after exposure to MS welding fume compared to air control (Table 3). However, significant increases were observed only for liver Fe and kidney Mn in the welding fume group compared to air control (Table 3). Cu levels in blood and other organs were measured, and no significant differences were observed. In the assessment of metal deposition in specific brain regions after welding fume inhalation, a significant increase in Mn concentration was observed in the cerebellum, cortex, and olfactory bulb at 1 day after 10 days of exposure to MS fume compared to air control (Fig. 2). Fe and Cu were not significantly elevated in any brain region after MS welding fume inhalation for 10 days (data not shown).

3.4. Expression of the divalent metal ion transporter 1

Following 10 days of exposure to MS welding fume a significant increase (1.5–2.3-fold) in the expression of the divalent metal ion transporter 1 (Dmt1) was observed in the dopaminergic targets, striatum and midbrain (Fig. 3).

Table 3
Metal concentrations in blood and organs.

Organ	Fe (μg/g dry tissue)	Mn (μg/g dry tissue)
Liver		
Air	232 ± 8.88	5.01 ± 0.23
Mild steel WF	284 ± 15.0[a]	5.43 ± 0.14
Heart		
Air	504 ± 74.6	1.24 ± 0.13
Mild steel WF	590 ± 86.9	1.58 ± 0.13
Kidney		
Air	192 ± 8.82	2.89 ± 0.16
Mild Steel WF	185 ± 15.6	3.35 ± 0.13[a]
Spleen		
Air	900 ± 80.1	0.94 ± 0.15
Mild Steel WF	963 ± 64.4	1.11 ± 0.11

Blood	Fe (μg/L)	Mn (μg/L)
Air	n.d.	8.27 ± 0.25
Mild steel WF	n.d.	9.92 ± 0.83

Note. Organ deposition of Fe and Mn at 1 day after inhalation of 40 mg/m^3 of mild steel welding fume (WF) for 3 h/day for 10 days. Cu levels in blood and other organs were measured, and no significant differences were observed. Control animals were exposed to filtered air. Values are means ± standard error (n = 5–6).
[a] Significantly greater than corresponding air control for a particular organ, $p < 0.05$; n.d. = not determined due to interference with heme iron present in blood.

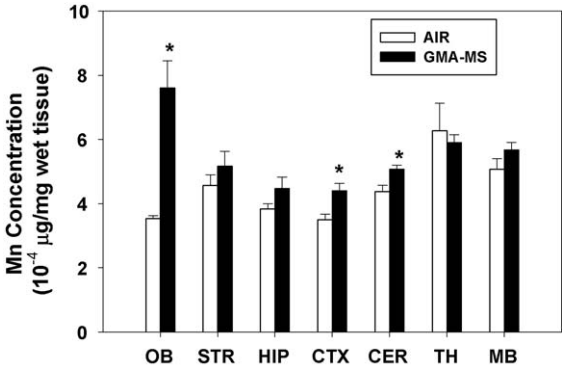

Fig. 2. Mn levels in specific brain regions at 1 day after inhalation of 40 mg/m^3 of gas metal arc-mild steel (GMA-MS) welding fume for 3 h/day for 10 days. Control animals were exposed to filtered air. Values are mean ± standard error. (*) Significantly greater than air controls for a particular brain region, $p < 0.05$ (n = 3).

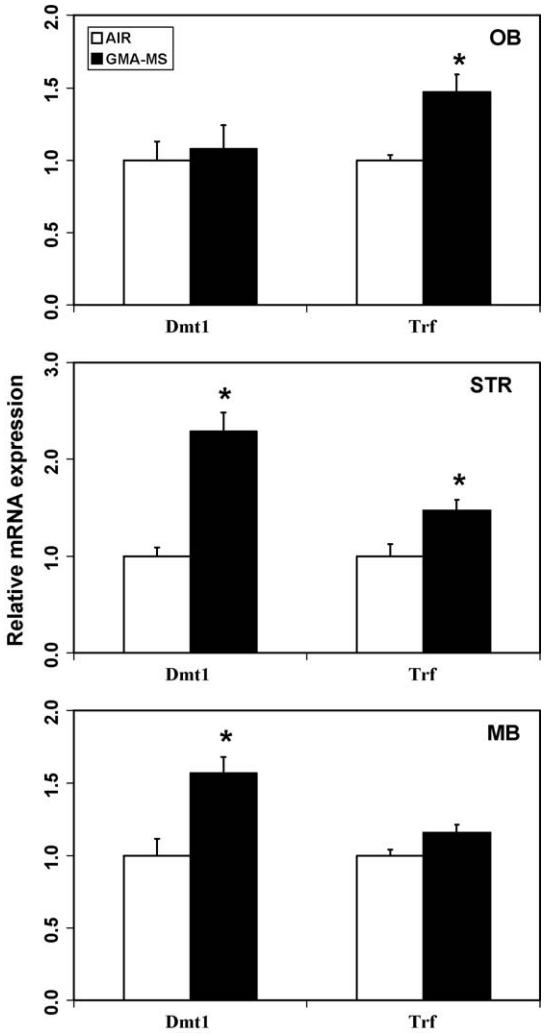

Fig. 3. Expression of divalent metal ion transporter 1 (Dmt1) in dopaminergic brain regions. Following 10 days of inhalation exposure to gas metal arc-mild steel (GMA-MS) welding fume, the mRNA expression of Dmt1 in olfactory bulb, striatum and midbrain was assayed by TaqMan® real-time PCR. The mRNA levels are expressed as fold change over corresponding air-exposed controls. Values are mean ± standard error. (*) Significantly different from air-exposed controls, $p < 0.05$ (n = 4–6 animals per group).

3.5. Brain region specific neuroinflammation and gliosis

Following 10 days of exposure to MS welding fume, a small but significant increase (~1.5-fold) in the expression of proinflammatory chemokines (Ccl2, Cxcl2) and cytokines (IL1β, TNFα) was observed, predominantly in the striatum, and is indicative of an early inflammatory response (Fig. 4). This proinflammatory response in the striatum was associated with a subtle increase (~1.5-fold) in the mRNA expression of the astroglial marker, GFAP (Fig. 5). Similarly, GFAP protein levels increased in the striatum and globus pallidus by 27% and 70%, respectively (Fig. 6). The induction of proinflammatory mediators and astrogliosis in the striatum and globus pallidus were consistent with an early insult in these basal ganglia targets.

3.6. Catecholamines

Although 10 days of exposure to MS welding fume resulted in increases in inflammatory cytokines as well as GFAP in the striatum and globus pallidus these indices of insult were not accompanied by any alterations in dopamine (Fig. 7) or its metabolites (data not shown). As Mn exposure may disrupt the regulation of GABAergic neurons (as reviewed by Gwiazda et al., 2002; Burton and Guilarte, 2009), additional HPLC analyses of these areas for GABA content indicated this exposure regimen had no effect on this biochemical parameter in rats (Fig. 7). A previous study observed that exposing non-human primates to chronic Mn produced about a 33% decrease, albeit non-significant, in globus pallidus GABA concentrations (Struve et al., 2007), while others have found no changes in GABAergic neurotransmitter systems (Burton et al., 2009).

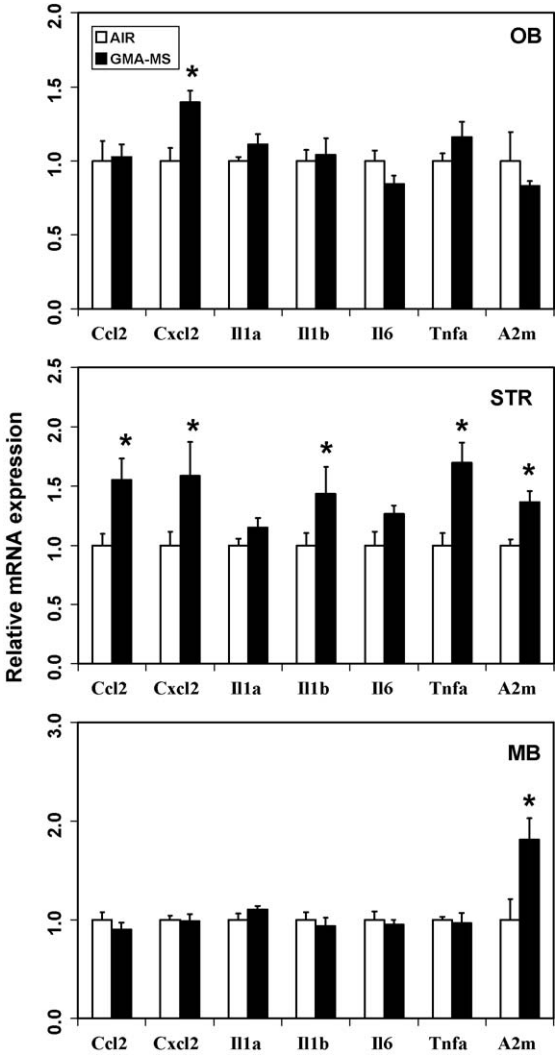

Fig. 4. Expression of neuroinflammatory chemokines and cytokines in dopaminergic brain regions. Following 10 days of inhalation exposure to gas metal arc-mild steel (GMA-MS) welding fume, the mRNA expression of proinflammatory chemokines and cytokines was assayed in olfactory bulb, striatum and midbrain by TaqMan® real-time PCR. The mRNA levels are expressed as fold change over corresponding air-exposed controls. Values are mean ± standard error. (*) Significantly different from air-exposed controls, $p < 0.05$ (n = 4–6 animals per group).

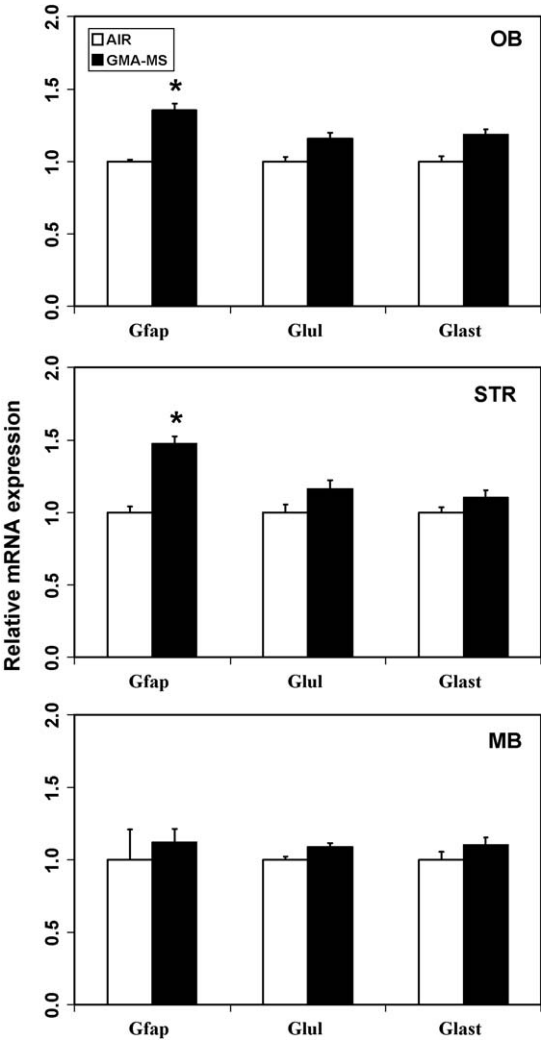

Fig. 5. Expression of glial responses in dopaminergic brain regions. Following 10 days of inhalation exposure to gas metal arc-mild steel (GMA-MS) welding fume, the mRNA expression of astroglial markers, GFAP, Glul and Glast was assayed in olfactory bulb, striatum and midbrain by TaqMan® real-time PCR. The mRNA levels are expressed as fold change over corresponding air-exposed controls. Values are mean ± standard error. (*) Significantly different from air-exposed controls, $p < 0.05$ (n = 4–6 animals per group).

3.7. Neuropathology

Ten days of inhalation to MS welding fume did not cause neurodegeneration in any brain regions as determined by histopathological analysis. Specific regional targets, the striatum and globus pallidus, were examined with increased interest as they showed subtle differences between control and welding fume treated animals by other measures (i.e., RNA). The striatum of welding fume-treated rats (Fig. 8B) appeared identical to control,

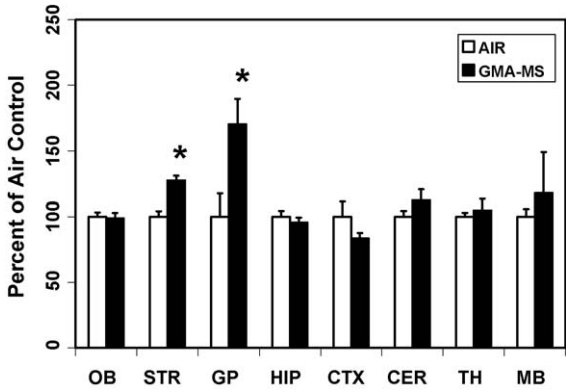

Fig. 6. Expression of GFAP protein in striatum and globus pallidus. Following 10 days of inhalation exposure to gas metal arc-mild steel (GMA-MS) welding fume, the levels of GFAP protein in discrete brain areas were measured by sandwich-ELISA. GFAP levels were calculated as μg/mg total protein and are expressed as % of air-exposed control. The basal levels of expression of GFAP in these brain areas vary and are as follows: OB = 2.84 ± 0.29, STR = 1.15 ± 0.16, GP = 2.66 ± 0.53, HIP = 3.50 ± 0.18, CTX = 1.51 ± 0.30, CER = 3.58 ± 0.17, TH = 2.38 ± 0.27 and MB = 1.46 ± 0.08 μg/mg total protein. Values are mean ± standard error. (*) Significantly different from air-exposed controls, $p < 0.05$ (n = 3–7 animals per group).

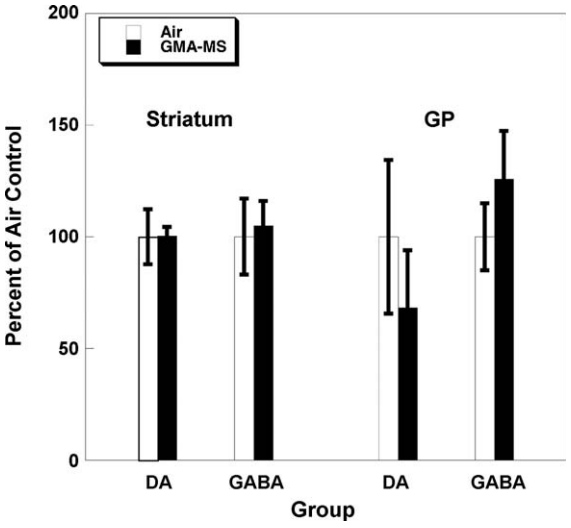

Fig. 7. Dopamine and GABA content of striatum (ST) and globus pallidus (GP). Following 10 days of inhalation exposure to air or gas metal arc-mild steel (GMA-MS) welding fume, the levels of DA and GABA were measured by HPLC following microwave euthanasia to insure stability. Data are expressed as the percent of the control value in the specific brain area. The basal levels of DA are 8.0 μg/g wet weight for ST and 45.1 pmol/total GP. The basal levels of GABA are 0.28 μg/g wet weight for ST and 0.45 μg/total GP. Values are mean ± standard error. Statistical analyses were performed on the raw values and revealed no effect of welding fume exposure.

air-treated animals (Fig. 8A). GFAP immunohistochemistry revealed no overt differences in astrocyte morphology between control (Fig. 8C) and welding fume-treated rats (Fig. 8D). Microglia stained by Iba-1 was observed in the ramified or resting state in both control (Fig. 8E) and welding fume-treated rats (Fig. 8F).

4. Discussion

The adverse health effects of occupational exposure to welding fumes have been a challenge to study due to diverse workplace settings and exposures to complex and varied aerosols generated from multiple welding processes. Among the recent concerns is the potential relationship between exposures to Mn-containing welding fumes and the development of parkinson-like neurological disorders (e.g., manganism, idiopathic PD). Due to the complexity of the exposures and workplace settings, delineating the causative factor in human exposures has often been confounding, thus calling for animal studies to evaluate the mechanistic basis of the potential neurotoxicity associated with welding fume inhalation. To investigate if welding fumes cause neurotoxicological effects, we evaluated the CNS effects in rats following whole-body inhalation exposure to MS welding fume, the most common type of welding process in the industry.

MS welding fume generated by the NIOSH robotic welding system was similar in size, composition, and morphology to MS welding fume generated in the workplace. The particles were mostly water-insoluble and composed primarily of a complex of Fe (80.6%) and Mn (14.7%). Particles were arranged as typical chain-like aggregates and had size distribution characteristics that extended from the ultrafine to fine-size range. A large portion of the inhaled MS particles were observed to be phagocytized by lung macrophages (Antonini et al., 2009). However, a large number of ultrafine particles in the size range below 0.1 μm are generated during welding. Because of the very short distance (~0.5 μm) between the alveolar spaces, where fume deposits, and the pulmonary capillary, some ultrafine particles may gain direct access to the bloodstream via uptake by alveolar type I cells that line the epithelium of the airspaces. The generation of such ultrafine particulates in welding increases the probability of these particles escaping phagocytosis in the lungs and translocating from pulmonary targets into the systemic circulation, and subsequently to other organ systems.

Further, there is potential for these aerosolized ultrafine particles to directly translocate to the brain via olfactory uptake mechanisms, involving the olfactory nerves. Indeed, aerosolized fine and nano-sized particles have been shown to translocate from olfactory regions or systemic circulation and accumulate in the brain (Hunter and Undem, 1999; Oberdorster et al., 2004; Elder et al., 2006). Also, there is evidence indicative of olfactory uptake of both soluble and non-soluble forms of Mn following intranasal (Tjalve et al., 1996), whole-body (Vitarella et al., 2000; Brenneman et al., 2000) or nose-only (Fechter et al., 2002) exposures. Fechter et al. (2002) have demonstrated that a 3-week nose-only exposure to non-soluble MnO_2 aerosols with a MMAD of 1.3 μm resulted in a significant elevation of olfactory bulb Mn concentrations. They also observed a small but non-significant increase in the striatal and cortical Mn concentrations upon exposure to these small particles. On the other hand, a larger size MnO_2 particle (18 μm) was not taken up by the olfactory nerves.

Consistent with the above findings, we observed significant accumulation of Mn in the olfactory bulb and small increases in the cortex and cerebellum following a 10-day exposure to MS welding fume. As described above, the MMAD of the welding particles generated by our system was 0.31 μm, which is well below the particle size that Fechter et al. (2002) used for their olfactory translocation studies. Taken together, these observations suggest that aerosolized welding fume particles in the size range of 1–2 μm or less have significant potential of being directly taken up via the olfactory pathway, independent of any extrapulmonary translocation. Because of the efficient uptake of intact particles that reach the circulation by Kupffer cells of the liver and the predominance of water-insoluble metals that compose the MS fume, it is possible that the translocation of these relatively non-soluble metal fume components occurs through olfactory uptake. The large accumulation of Mn in the olfactory bulb is suggestive of such an occurrence.

However, Fe concentrations remained unchanged in the olfactory bulb and other brain region when comparing the welding fume and air control groups. Because welding fumes are a complex mixture of different metals, this observation would tend to suggest a differential solubilization of the Fe and Mn from the particles. It

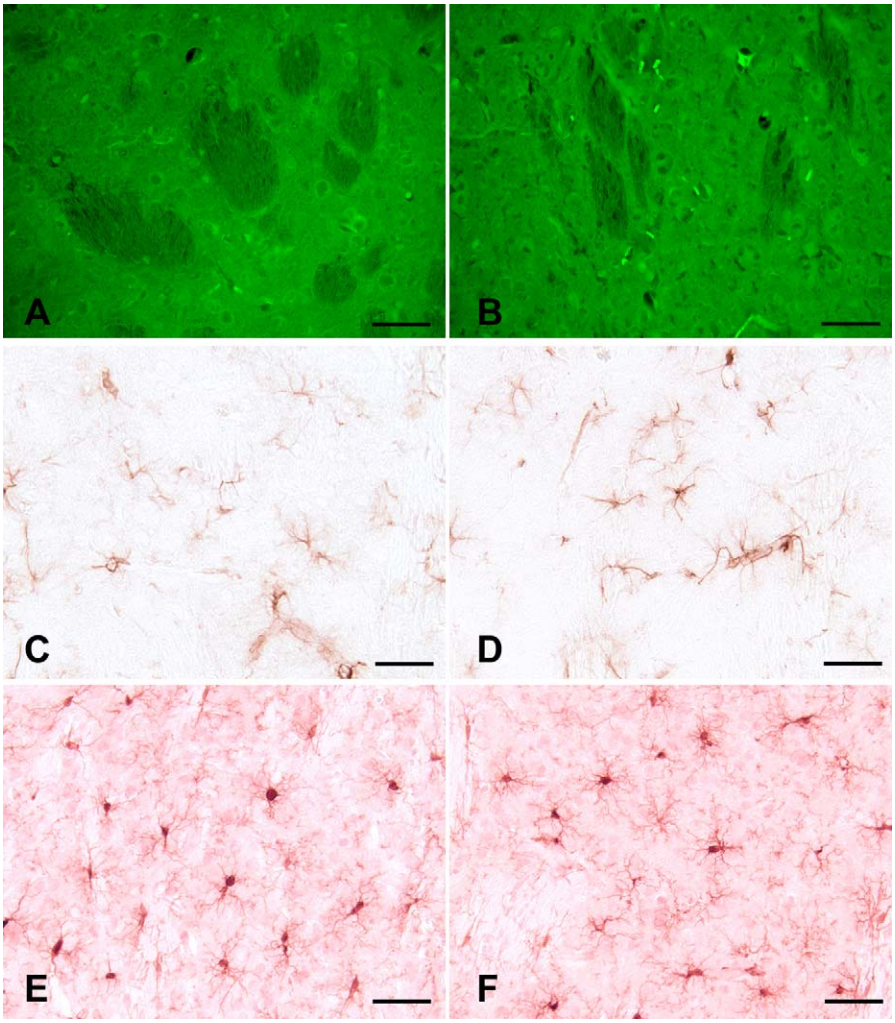

Fig. 8. Neuropathology of specific brain regions. Fluoro-Jade B, a fluorescent marker for the identification of neuronal damage showed no differences between air (A) and mild steel welding fume (B) treatments in a specific regional target, the striatum. Astrocytes were not activated in response to neuronal damage and appeared similar between air (C) and welding fume (D) treatments. Microglia were observed in the resting state in both air (E) and welding fume (F) treated animals, indicating no significant activation of this cell population. Scale bar = 50 μm.

has been observed that soluble Fe, unlike soluble Mn, may not be transported to the rat brain via olfactory uptake (Rao et al., 2003). An alternative hypothesis that may explain the differential uptake of Mn and Fe in the olfactory bulb may be related to the presence of large numbers of ultrafine particles generated during welding. Some of these ultrafine particles may be more enriched with one metal (e.g., Mn) as opposed to a complex of multiple metals, allowing for preferential olfactory uptake of intact particles composed of a specific element. This possibility is being investigated by our group and others using advanced electron microscopic methodologies.

In a recent commentary, Ghio and Bennett (2007) question the translocation of intact metal particles after deposition in the respiratory tract. They argue that elevated concentrations of metal in extrapulmonary tissues do not prove direct translocation of metal particles, but rather reflect solubilization and mobilization of specific metals from particles. Also, the rapidity of change in metal concentration at an extrapulmonary site does not necessarily support a direct translocation because the time required for solubilization, mobilization, and systemic transport have not been defined. The required time for solubilization may be short for ultrafine particles, which have an increased surface area.

It is important to appreciate that welding fumes are a complex of different metals, and the bioavailability of the individual metals in welding fumes may differ compared to the bioavailability of a single metal that has deposited in the lungs. Lam et al. (1979) observed that the removal of certain metallic components of the fume after deposition in the lungs occurred in three phases, each dependent on the *in vivo* solubility of the specific metal. Phase I represented mucociliary clearance of deposited particles as the eliminated metal constituents appeared in the fecal material with quick elimination half-times of less than 1 day. The clearance rates of each element of the fume were similar during this initial phase, indicating that the eliminated particles were transported in their entirety, without separation of the constituents. Phase II was a slower process with a retention half-time of up to a week. The clearance rates for the various welding fume components were very consistent, indicating that the particles were still being transported in an unchanged state. Phase III was a much slower process with the welding constituents having biological half-times of several weeks. Unlike phases I and II, the various elements of a particular fume were cleared from the lungs at very different rates, indicating a separation of the material during phase III which was attributable to the solubility in tissue of each metal present in the welding fume. It appears from the findings of our current study that some solubilization of deposited particles is occurring over the 10-day exposure period. Significant elevations in kidney Mn and liver Fe were observed at the time of sacrifice. Importantly, we

have observed that Mn and Fe are cleared from the lungs at different rates after pulmonary exposure to welding fumes (unpublished results). In addition, different rates and mechanisms of elimination from the body may be occurring for each metal. Tapin et al. (2006) did not observe a concentration-dependent increase of Mn in the liver, supporting enhanced biliary excretion of Mn after inhalation.

It is important to mention that olfactory transport is a rapid means of Mn uptake by brain structures in the rat (Gianutsos et al., 1997; Brenneman et al., 2000). However, because of interspecies differences between rats and humans in nasal and brain anatomy, the relevance of these findings to human Mn inhalation exposure and the risks for neurotoxicity are unknown (Brenneman et al., 2000). In the rat, the olfactory bulb accounts for a significantly larger portion of the central nervous system as compared to humans. Rats also are obligatory nasal breathers, whereas humans are oronasal breathers. It has been reported that only about 5% of the inhaled air stream reaches the olfactory region in humans (Kimbell et al., 1997). Because of these anatomic and physiological differences, rats may be more prone to olfactory deposition and transport of Mn and other inhaled toxicants when compared to humans. It is also important to note that the neurobehavioral toxicity of Mn may vary in rodents depending on the form of Mn and the route of administration and has not completely modeled the changes seen in humans (Boyes and Miller, 1998; Aschner et al., 2007).

Despite the potential relevance issues related to rat-to-human extrapolations, exposure to MS welding fume induced the expression of the divalent metal transporter-1 (Dmt1) in dopaminergic brain areas in rats. These observations suggest that sequestration of soluble divalent metals into neural cells can occur in these brain regions. The selective expression of Dmt1 and the associated proinflammatory and glial responses in the dopaminergic targets provide preliminary evidence to suggest that MS welding fume exposure has the potential to damage neural elements of the basal ganglia. Activated microglia and astrocytes are known to play an important role in elaboration of neuroinflammatory responses (Raivich et al., 1996; Ransohoff et al., 1996; Ubogu et al., 2006), including enhanced expression of proinflammatory chemokines and cytokines (De Bock et al., 1996; Botchkina et al., 1997; Sriram et al., 2002; Sriram and O'Callaghan, 2005, 2007). While proinflammatory chemokines and cytokines have been linked to a variety of neurodegenerative disease conditions (Bauer et al., 1991; Boka et al., 1994; Mogi et al., 1996; Hirsch and Hunot, 2009), genetic or pharmacological suppression of neuroinflammation following toxicant-induced neuronal damage does not necessarily result in modulation of neuronal damage and astrogliosis (O'Callaghan et al., 2008). Not surprisingly, therefore, neuroinflammatory reactions in the brain have been proposed to play both deleterious and trophic roles in neural damage and brain disease (Raivich et al., 1996). It is possible that the neuroinflammatory changes following short-term MS welding fume exposure may be an acute adaptive response to a systemic insult. On the other hand, such responses may be indicative of early neural changes that precede overt neuropathology. The selective accumulation of Mn and the small rise in GFAP mRNA and protein, a dominant response of astrocytes to all types of neurotoxic insults (O'Callaghan and Sriram, 2005), are consistent with this view. While the astroglial responses may reflect subtle underlying neuronal damage not detectable by Fluoro-Jade staining, such damage would not involve dopaminergic neurons, the target of concern for PD. Otherwise, decrements in striatal dopamine or its metabolites would have been observed along with the elevations in GFAP mRNA and protein (O'Callaghan et al., 2008).

With our animal model, an attempt is being made to examine whether the subtle changes in neuroinflammation may be predictors for the potential development of later neurological decrements after exposure to Mn-containing welding fumes. These and other evaluations of early molecular or biochemical changes are critical for the development of efficient biomonitoring and intervention methods to prevent adverse neurological health effects related to welding fume exposure. In concert, long-term inhalation exposure studies to evaluate potential neuropathological and neurobehavioral alterations are currently ongoing.

In summary, our goal was to develop an animal model to measure the accumulation of Mn in specific brain areas and to examine the potential neurological responses associated with the inhalation of MS welding fume. Short-term exposure to high concentrations of MS fume led to an accumulation of Mn in the olfactory bulb, cerebellum, and cortex. The mechanisms (e.g., olfactory uptake of intact particles vs. solubilization of metals) by which Mn reaches specific brain regions after welding fume inhalation are still to be determined. There was no evidence of observable changes in neuronal cell injury as assessed by histopathology. However, subtle changes in cell markers of neuroinflammatory and astrogliosis were observed. The neurofunctional significance of these findings currently is being investigated in longer, more chronic welding fume exposure studies.

DISCLAIMER

The findings and conclusions of this paper have not been formally disseminated by NIOSH and should not be construed to represent any agency determination or policy.

Acknowledgments

The authors wish to acknowledge the expert technical assistance on the project of Michelle Donlin, Amy Frazer, and Jared Cumpston from the inhalation exposure team. The authors thank Mark Millson from the Division of Applied Research and Technology in NIOSH for performing inductively coupled plasma atomic absorption spectroscopy for the project. The authors also wish to thank the National Toxicology Program, the Manganese Health Research Program, and Dr. Richard Dey of West Virginia University for additional support and collaboration during the ongoing welding project.

References

Antonini JM. Health effects of welding. Crit Rev Toxicol 2003;33:61–103.
Antonini JM, Santamaria AB, Jenkins NT, Albini E, Lucchini R. Fate of manganese associated with the inhalation of welding fumes: potential neurological effects. Neurotoxicology 2006a;27:304–10.
Antonini JM, Afshari AA, Stone S, Chen BT, Scwegler-Berry D, Fletcher WG, et al. Design, construction, and characterization of a novel robotic welding fume generator and inhalation exposure system for laboratory animals. J Occup Environ Hyg 2006b;3:194–203.
Antonini JM, Roberts JR, Stone S, Chen BT, Schwegler-Berry D, Frazer DG. Short-term inhalation exposure to mild steel welding fume had no effect on lung inflammation and injury, but did alter defense responses to bacteria in rats. Inhal Toxicol 2009;21:182–92.
Aschner M, Guilarte TR, Schneider JS, Zheng W. Manganese: recent advances in understanding its transport and neurotoxicity. Toxicol Appl Pharmacol 2007;221:131–47.
AVMA Panel on Euthanasia. American Veterinary Medical Association. 2000 report of the AVMA Panel on Euthanasia. J Am Vet Med Assoc 2001;218:669–96.
Bauer J, Strauss S, Schreiter-Gasser U, Ganter U, Schlegel P, Witt I, et al. Interleukin-6 and alpha-2-macroglobulin indicate an acute-phase state in Alzheimer's disease cortices. FEBS Lett 1991;285:111–4.
Botchkina GI, Meistrell ME, Botchkina IL, Tracey KJ. Expression of TNF and TNF receptors (p55 and p75) in the rat brain after focal cerebral ischemia. Mol Med 1997;3:765–81.
Boka G, Anglade P, Wallach D, Javoy-Agid F, Agid Y, Hirsch EC. Immunocytochemical analysis of tumor necrosis factor and its receptors in Parkinson's disease. Neurosci Lett 1994;172:151–4.
Bowler RM, Gysens S, Diamond E, Booty A, Hartney C, Roels HA. Neuropsychological sequelae of exposure to welding fumes in a group of occupationally exposed men. Int J Hyg Environ Health 2003;206:517–26.
Bowler RM, Nakagawa S, Drezgic M, Roels HA, Park RM, Diamond E, et al. Sequelae of fume exposure in confined space welding: a neurological and neuropsychological case series. Neurotoxicology 2007a;28:298–311.

Bowler RM, Roels HA, Nakagawa S, Drezgic M, Diamond E, Park R, et al. Dose–effect relationships between manganese exposure and neurological, neuropsychological and pulmonary function in confined space bridge welders. Occup Environ Med 2007b;64:167–77.
Boyes WK, Miller DB. A review of rodent models of manganese neurotoxicity. Neurotoxicology 1998;19:468.
Brenneman KK, Wong BA, Buccellato MA, Costa ER, Gross EA, Dorman DC. Direct olfactory transport of inhaled manganese $^{54}MnCl_2$ to the rat brain: toxicokinetic investigations in a unilateral nasal occlusion model. Toxicol Appl Pharmacol 2000;169:238–48.
Bureau of Labor Statistics. Occupational employment statistics: occupational employment and wages, 2007, cutter, solders, and brazers. U.S. Department of Labor; 2007 Available at: http://www.bls.gov/oes/current/oes514121.htm. Accessed 11/10/2008.
Burton NC, Guilarte TR. Manganese neurotoxicity: lesson learned from longitudinal studies in nonhuman primates. Environ Health Perspect 2009;117:325–32.
Burton NC, Schneider JS, Syversen T, Guilarte TR. Effects of chronic manganese exposure on glutamatergic and GABAergic markers in the nonhuman primate brain. Toxicol Sci 2009;111:131–9.
Calne DB, Chu NS, Huang CC, Lu CS, Olanow W. Manganism and idiopathic parkinsonism: similarities and differences. Neurology 1994;44:1583–6.
Coggon D, Inskip H, Winter P, Pannett B. Occupational mortality of men. London: Medical Research Council; 1995 p. 23–261.
De Bock F, Dornand J, Rondouin G. Release of TNF alpha in the rat hippocampus following epileptic seizures and excitotoxic neuronal damage. Neuroreport 1996;7:1125–9.
Discalzi G, Pira E, Hernandez EH, Valentina C, Turbiglio M, Meliga F. Occupational manganese parkinsonism: magnetic resonance imaging and clinical patterns flowing $CaNa_2$–EDTA chelation. Neurotoxicology 2000;21:863–6.
Dobson AW, Erikson KM, Aschner M. Manganese neurotoxicity. Ann NY Acad Sci 2004;1012:115–28.
Elder A, Gelein R, Silva V, Feikert T, Opanashuk L, Carter J, et al. Translocation of inhaled ultrafine manganese oxide particles to the central nervous system. Environ Health Perspect 2006;114:1172–8.
Ellingsen DG, Konstantinov R, Bast-Pettersen R, Merkurjeva L, Chashchin M, Thomassen Y, et al. A neurobehavioral study of current and former welders exposed to manganese. Neurotoxicology 2008;29:48–59.
Fechter LD, Johnson DL, Lynch RA. The relationship of particle size to olfactory nerve uptake of a non-soluble form of manganese into brain. Neurotoxicology 2002;23:177–83.
Fored CM, Fryzek JP, Brandt L, Nise G, Sjogren B, McLaughlin JK, et al. Parkinson's disease and other basal ganglia or movement disorders in a large nationwide cohort of Swedish welders. Occup Environ Med 2006;63:135–40.
Franek B. Manganese exposure during welding operations. Appl Occup Environ Hyg 1994;9:537–8.
Fryzek JP, Hansen J, Cohen S, Bonde JP, Llambias MT, Kolstad HA, et al. A cohort study of Parkinson's disease and other neurodegenerative disorders in Danish welders. J Occup Environ Med 2005;47:466–72.
Ghio AJ, Bennett WD. Metal particles are inappropriate for testing a postulate of extrapulmonary transport. Environ Health Perspect 2007;115:A70.
Gianutsos H, Morrow GR, Morris JB. Accumulation of manganese in rat brain following intranasal administration. Fundam Appl Toxicol 1997;37:102–5.
Goldman SM, Tanner CM, Olanow CW, Watts RL, Field RD, Langston JW. Occupation and parkinsonism in three movement disorders clinics. Neurology 2005;65:1430–5.
Gwiazda RH, Lee D, Sheridan J, Smith DR. Low cumulative manganese exposure affects striatal GABA but not dopamine. Neurotoxicology 2002;23:69–76.
Hirsch EC, Hunot S. Neuroinflammation in Parkinson's disease: a target for neuroprotection. Lancet Neurol 2009;8:382–97.
Hunter DD, Undem BJ. Identification and substance P content of vagal afferent neurons innervating the epithelium of the guinea pig trachea. Am J Respir Crit Care Med 1999;159:1943–8.
Jankovic J. Searching for a relationship between manganese and welding and Parkinson's disease. Neurology 2005;64:2021–8.
Josephs KA, Ahlskog JE, Klos KJ, Kumar N, Fealey RD, Trenerry MR, et al. Neurologic manifestations in welders with pallidal MRI T1 hyperintensity. Neurology 2005;64:2033–9.
Kim Y, Kim J-W, Ito K, Lim H-S, Cheong H-K, Kim JY, et al. Idiopathic parkinsonism with superimposed manganese exposure: utility of positron emission tomography. Neurotoxicology 1999;20:249–52.
Kim E, Kim Y, Cheong HK, Cho S, Shin YC, Sakong J, et al. Pallidal index on MRI as a target organ dose of manganese: structural equation analysis. Neurotoxicology 2005;26:351–9.
Kimbell JS, Godo MN, Gross EA, Joyner DR, Richardson RB, Morgan KT. Computer simulation of inspiratory airflow in all regions of the F344 rat nasal passages. Toxicol Appl Pharmacol 1997;145:388–98.
Lam HF, Hewitt PJ, Hicks R. A study of pulmonary deposition, and the elimination of some constituent metals from welding fume in laboratory animals. Ann Occup Hyg 1979;21:363–73.
Lehman EJ, Hein MJ, Estill CF. Proportionate mortality study of the United Association of Journeymen and Apprentices of the Plumbing and Pipe Fitting Industry. Am J Ind Med 2008;51:950–63.
Marsh GM, Gula MJ. Employment as a welder and Parkinson's disease among heavy equipment manufacturing workers. J Occup Environ Med 2006;48:1031–46.
McMillan DE. A brief history of the neurobehavioral toxicity of manganese: some unanswered questions. Neurotoxicology 1999;20:499–507.
Mogi M, Harada M, Narabayashi H, Inagaki H, Minami M, Nagatsu T. Interleukin (IL)-1 beta, IL-2, IL-4, IL-6 and transforming growth factor-alpha levels are elevated in ventricular cerebrospinal fluid in juvenile Parkinsonism and Parkinson's disease. Neurosci Lett 1996;211:13–6.
Nelson K, Golnick J, Korn T, Angle C. Manganese encephalopathy: utility of early magnetic resonance imaging. Br J Ind Med 1993;50:510–3.
NIOSH. Elements (ICP): method 7300. In: NIOSH manual of analytical methods. 4th ed., issue 2 Washington, DC: U.S. Department of Health and Human Services/NIOSH; 1994 Publication No. 98–119.
NIOSH. Welding and manganese: potential neurological effects. National Institute for Occupational Safety and Health; 2009 Available at: http://www.cdc.gov/niosh/topics/welding Accessed 04/21/2009.
Oberdorster G, Sharp Z, Atudorei V, Elder A, Gelein R, Kreyling W, et al. Translocation of inhaled ultrafine particles to the brain. Inhal Toxicol 2004;16:437–45.
O'Callaghan JP. Quantification of glial fibrillary acidic protein: comparison of slot-immunobinding assays with a novel sandwich ELISA. Neurotoxicol Teratol 1991;13:275–81.
O'Callaghan JP. Measurement of glial fibrillary acidic protein. In: Maines MD, Costa LG, Hodgson E, Reed DJ, Sipes IG, editors. Current protocols in toxicology. New York: John Wiley & Sons; 2002 p. 12.81.1–12.8.12.
O'Callaghan JP, Sriram K. Glial fibrillary acidic protein and related glial proteins as biomarkers of neurotoxicity. Expert Opin Drug Saf 2005;4:433–42.
O'Callaghan JP, Sriram K, Miller DB. Defining "neuroinflammation". Ann NY Acad Sci 2008;1139:318–30.
Pal PK, Samii A, Calne DB. Manganese neurotoxicity: a review of clinical features, imaging, and pathology. Neurotoxicology 1999;20:227–38.
Park J, Yoo C-I, Sim CS, Kim JW, Yi Y, Shin YC, et al. A retrospective cohort study of Parkinson's disease in Korean shipbuilders. Neurotoxicology 2006;27:445–9.
Park RM, Schulte PA, Bowman JD, Walker JT, Bondy SC, Yost MG, et al. Potential occupational risks for neurodegenerative diseases. Am J Ind Med 2005;48:63–77.
Perl DP, Olanow CW. The neuropathology of manganese-induced parkinsonism. J Neuropathol Exp Neurol 2007;66:675–82.
Racette BA, McGee-Minnich L, Moerlein SM, Mink JW, Videen TO, Perlmutter JS. Welding-related parkinsonism: clinical features, treatment, and pathophysiology. Neurology 2001;56:8–13.
Raivich G, Bluethmann H, Kreutzberg GW. Signaling molecules and neuroglial activation in the injured central nervous system. Keio J Med 1996;45:239–47.
Ransohoff RM, Glabinski A, Tani M. Chemokines in immune-mediated inflammation of the central nervous system. Cytokine Growth Factor Rev 1996;7:35–46.
Rao DB, Wong BA, McManus BE, McElveen AM, James AR, Dorman DC. Inhaled iron, unlike manganese, is not transported to the rat brain via olfactory pathway. Toxicol Appl Pharmacol 2003;193:116–26.
Sadek AH, Rauch R, Schulz PE. Parkinsonism due to manganism in a welder. Int J Toxicol 2003;22:393–401.
Schmued LC, Hopkins KJ. Fluoro-Jade B: a high affinity fluorescent marker for the localization of neuronal degeneration. Brain Res 2000;874:123–30.
Sinczuk-Walczak H, Jakubowski M, Matczak W. Neurological and neurophysiological examinations of workers occupationally exposed to manganese. Int J Occup Med Environ Health 2001;14:329–37.
Sjogren B, Gustavsson P, Hogstedt C. Neuropsychiatric symptoms among welders exposed to neurotoxic metals. Br J Ind Med 1990;47:704–7.
Sjogren B, Iregren A, Frech W, Hagman M, Johansson L, Tesarz M, et al. Effects of the nervous system among welders exposed to aluminum and manganese. Occup Environ Med 1996;53:32–40.
Sriram K, Matheson JM, Benkovic SA, Miller DB, Luster MI, O'Callaghan JP. Mice deficient in TNF receptors are protected against dopaminergic neurotoxicity: implications for Parkinson's disease. FASEB J 2002;16:1474–6.
Sriram K, O'Callaghan JP. Signaling mechanisms underlying toxicant-induced gliosis. In: Aschner M, Costa LG, editors. The role of glia in neurotoxicity 2nd ed. Boca Raton, FL: CRC Press; 2005141–71.
Sriram K, O'Callaghan JP. Divergent roles for tumor necrosis factor-α in the brain. J Neuroimmune Pharmacol 2007;2:140–53.
Stampfer MJ. Welding occupations and mortality from Parkinson's disease and other neurodegenerative diseases among United States men, 1985–1999. J Occup Environ Hyg 2009;6:267–72.
Struve MF, McManus BE, Wong BA, Dorman DC. Basal ganglia neurotransmitter concentrations in Rhesus monkeys following subchronic manganese sulfate inhalation. Am J Ind Med 2007;50:772–8.
Tapin D, Kennedy G, Lambert J, Zayed J. Bioaccumulation and locomotor effects of manganese sulfate in Sprague–Dawley rats following subchronic (90 days) inhalation exposure. Toxicol Appl Pharmacol 2006;211:166–74.
Tjalve H, Henriksson J, Tallkvist J, Larsson BS, Lindquist NG. Uptake of manganese and cadmium from nasal mucosa into the central nervous system via olfactory pathways in rats. Pharmacol Toxicol 1996;79:347–56.
Ubogu EE, Cossoy MB, Ransohoff RM. The expression and function of chemokines involved in CNS inflammation. Trends Pharmacol Sci 2006;27:48–55.
Vitarella D, Wong BA, Moss OR, Dorman DC. Pharmacokinetcis of inhaled manganese phosphate in male Sprague–Dawley rats following subacute (14 days) exposure. Toxicol Appl Pharmacol 2000;163:279–85.
Wang J-D, Huang C-C, Hwang Y-H, Chiang J-R, Lin J-M, Chen J-S. Manganese induced parkinsonism: an outbreak due to unrepaired ventilation control system in a ferromanganese smelter. Br J Ind Med 1989;46:856–9.